^{131}I-IITM and ^{211}At-AITM: Two Novel Small-Molecule Radiopharmaceuticals Targeting Oncoprotein Metabotropic Glutamate Receptor 1

Lin Xie*[1], Masayuki Hanyu*[1], Masayuki Fujinaga[1], Yiding Zhang[1], Kuan Hu[1], Katsuyuki Minegishi[1], Cuiping Jiang[1], Fuki Kurosawa[1,2], Yukie Morokoshi[2], Huizi Keiko Li[2,3], Sumitaka Hasegawa[2], Kotaro Nagatsu[1], and Ming-Rong Zhang[1]

[1]Department of Advanced Nuclear Medicine Sciences, National Institute of Radiological Sciences, National Institutes for Quantum and Radiological Science and Technology, Chiba, Japan; [2]Department of Charged Particle Therapy Research, National Institute of Radiological Sciences, National Institutes for Quantum and Radiological Science and Technology, Chiba, Japan; and [3]The Japan Society for the Promotion of Science, Tokyo, Japan

Targeted radionuclide therapy (TRT) targeting oncoproteins facilitates the delivery of therapeutic radionuclides to tumor tissues with high precision. Herein, we developed 2 new radiopharmaceuticals, 4-^{131}I-iodo- and 4-^{211}At-astato-*N*-[4-(6-(isopropylamino)pyridine-4-yl)-1,3-thiazol-2-yl]-*N*-methylbenzamide (^{131}I-IITM and ^{211}At-AITM), targeting the ectopic metabotropic glutamate receptor 1 (mGluR1) in melanomas for TRT studies. **Methods:** ^{131}I-IITM and ^{211}At-AITM were synthesized by reacting a stannyl precursor with ^{131}I-NaI and ^{211}At in the presence of an oxidizing agent. The therapeutic efficacy and safety of the 2 radiopharmaceuticals were investigated using mGluR1-expressing B16F10 melanoma cells and melanoma-bearing mice. **Results:** ^{131}I-IITM and ^{211}At-AITM were obtained with a radiochemical purity of greater than 99% and radiochemical yields of 42.7% ± 10.4% and 45.7% ± 6.5%, respectively, based on the total radioactivity of used radionuclides. ^{131}I-IITM and ^{211}At-AITM exhibited a maximum uptake of 4.66% ± 0.70 and 7.68% ± 0.71 percentage injected dose per gram (%ID/g) in the targeted melanomas, respectively, and were rapidly cleared from nontarget organs after intravenous injection. Both agents markedly inhibited melanoma growth compared with the controls (61.00% and 95.68%, respectively). In the melanoma model, considerably greater therapeutic efficacy with negligible toxicity was observed using ^{211}At-AITM. **Conclusion:** The nontoxic radiopharmaceuticals ^{131}I-IITM and ^{211}At-AITM are useful high-precision TRT agents that can be used to target the oncoprotein mGluR1 for melanoma therapy.

Key Words: small-molecule radiopharmaceutical; oncoprotein; metabotropic glutamate receptor 1 (mGluR1); melanoma; targeted radionuclide therapy (TRT)

J Nucl Med 2020; 61:242–248
DOI: 10.2967/jnumed.119.230946

Unlike conventional external beam therapy, targeted radionuclide therapy (TRT) with radiopharmaceuticals allows carriers to deliver therapeutic radionuclides to diagnosed neoplastic malformations, metastasized cells, and cellular clusters, providing systemic radiotherapy for cancer (*1*). A carrier–radionuclide pair that combines the specificity of a carrier with potent cytotoxic radiation can facilitate the targeting of tumors with high precision (*2*). The carrier agents are designed as antibodies, proteins, peptides, and small molecules, and facilitate tumor cell targeting with α-, β-, and Auger electron-emitting radionuclides that have unique physicochemical properties (*3*). Although, to date, TRT using antibody-based radiopharmaceuticals has shown impressive clinical responses in patients with hematologic malignancies, its therapeutic effect is somewhat less pronounced when used against most solid tumors, including melanomas (*4–7*). To overcome this deficiency and broaden the therapeutic scope of TRT, small-molecule–based radiopharmaceuticals have attracted considerable attention due to their favorable pharmacokinetics, stability, versatility, and amenability to derivatization (*2,8*).

In this study, we aimed to develop 2 new small-molecule TRT radiopharmaceuticals, 4-^{131}I-iodo- and 4-^{211}At-astato-*N*-[4-(6-(isopropylamino)pyrimidin-4-yl)-1,3-thiazol-2-yl]-*N*-methylbenzamide (^{131}I-IITM and ^{211}At-AITM, respectively; Fig. 1), targeting metabotropic glutamate receptor type 1 (mGluR1) in melanomas. Ectopic mGluR1 has oncogenic characteristics that independently drive the carcinogenesis of melanocytes with 100% penetrance (*9*). Although the oncoprotein mGluR1 is not expressed in normal skin, benign nevi, or peripheral organs, it is expressed in the central nervous system and has been found to be ectopically expressed in 68%–80% of human melanoma biopsy specimens (*9,10*). Moreover, it is widely detected in carcinomas of the breast, prostate, colon, and lung (*11*).

We previously developed 4-^{18}F-fluoro-*N*-[4-[6-(isopropylamino) pyrimidin-4-yl]-1,3-thiazol-2-yl]-N-methylbenzamide (^{18}F-FITM; Fig. 1) to visualize and quantify mGluR1 expression in the brain (*12,13*) and melanomas (*14*). This radiotracer is a specific antagonist for mGluR1, with a half maximal inhibitory concentration (IC_{50}) value of 5.1 nM, and displays excellent selectivity for mGluR1 compared with other subtypes ($IC_{50} > 7$ μM). PET studies using ^{18}F-FITM have demonstrated that mGluR1 may become an important target for clinical development, including personalized diagnosis and treatment of melanomas (*14*). ^{131}I-IITM and ^{211}At-AITM are 2 halogen analogs derived from ^{18}F-FITM. In preliminary studies, we labeled IITM with ^{11}C and found that replacement of the smaller fluorine atom by the larger iodine atom prevented ^{11}C-IITM (Fig. 1) entrance into the mGluR1-rich brain, while simultaneously

Received May 9, 2019; revision accepted Jul. 31, 2019.
For correspondence or reprints contact: Ming-Rong Zhang, Department of Advanced Nuclear Medicine Sciences, 4-9-1 Anagawa, Inage-Ku, Chiba, Japan;
E-mail: zhang.ming-rong@qst.go.jp
*Contributed equally to this work.
Published online Aug. 26, 2019.

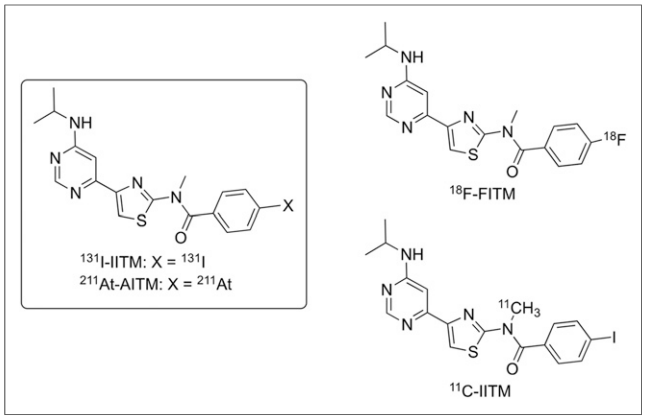

FIGURE 1. Chemical structures of ^{131}I-IITM and ^{211}At-AITM derived from ^{18}F-FITM and ^{11}C-IITM.

maintaining high tumor uptake and specificity for mGluR1 (*15*), which is a prerequisite for developing radiolabeled IITM for cancer radiotherapy. These findings motived us to label IITM with the β-emitting nuclide ^{131}I, the most used halogen isotope, and the α-emitting nuclide ^{211}At, which has halogen properties similar to ^{131}I. Here, we evaluated the utility of ^{131}I-IITM and ^{211}At-AITM for TRT studies by investigating their therapeutic efficacy and safety in mGluR1-expressing B16F10 melanoma cells and melanoma-bearing mice.

MATERIALS AND METHODS

Radiosynthesis

Radiosynthesis of ^{131}I-IITM or ^{211}At-AITM was performed by reacting a stannyl precursor (100 μg) with ^{131}I-NaI or ^{211}At in the presence of oxidizing agent (supplemental materials; supplemental materials are available at http://jnm.snmjournals.org). The radioactive reaction mixture was separated by reverse-phase high-performance liquid chromatography to obtain ^{131}I-IITM (260 GBq/μmol molar activity) or ^{211}At-AITM for use in different experiments. Radiochemical purity was analyzed using high-performance thin-layer chromatography and high-performance liquid chromatography.

Tumor Cell Lines, Mice, and Mouse Models

Transplantable B16Fl0 melanoma cells from C57BL/6J mice were obtained from the American Type Culture Collection. Previously, immunohistochemical analysis has verified the abundance of ectopic mGluR1 on the surface of B16F10 melanomas (*14,15*). The B16Fl0 cells were maintained and passaged in Dulbecco's modified Eagle's medium supplemented with 10% fetal bovine serum, penicillin (100 U/mL), and streptomycin (0.1 mg/mL). Periodic polymerase chain reaction (Takara Bio) analyses indicated that the cells were free of bacterial contaminants, including mycoplasmas.

Animal experiments were performed using 6- to 8-wk-old male C57BL/6J mice (Japan SLC). The melanoma models were created by injecting a single-cell suspension of 5×10^4 B16F10 cells in 100 μL of Dulbecco's modified Eagle's medium without serum into the left flank of C57BL/6J mice. On day 7 after subcutaneous inoculation, mice with a maximum tumor diameter of approximately 5 mm were selected for further studies. All animal studies were approved by the Animal Ethics Committee of the National Institutes for Quantum and Radiologic Science and Technology (QST). The animals were maintained and handled in accordance with the recommendations of the National Institute of Health and QST institutional guidelines.

Binding Ability

B16F10 melanoma cells (5×10^4 cells) were seeded in 24-well plates and allowed to form an adherent culture overnight for further experiments. To examine the binding ability of these cells, they were incubated with increasing doses of ^{131}I-IITM (0, 0.5, 1.0, 1.5, 2.0, and 2.5 MBq/mL) at 37°C for 18 h. To determine the biospecificity of ^{131}I-IITM (2.5 MBq/mL) and ^{211}At-AITM (25 kBq/mL), they were added to cultures with or without unlabeled FITM (10 μmol/L) at 37°C for 18 h. Cell culture supernatants were removed, and the cells were washed with phosphate-buffered saline (PBS) and dissolved in 0.2 mol/L NaOH. Radioactivity was measured using a γ-counter (PerkinElmer). The protein content of cell lysates was quantified using a protein assay kit (Bio-Rad). Cellular uptake was calculated as a percentage of the incubated radioactivity normalized per mg protein (%ICD/mg protein).

Cytotoxicity

B16F10 cells were cultured with medium only (control group), ^{131}I-IITM (2.5 MBq/mL), or ^{211}At-AITM (25 kBq/mL) at 37°C. After 18 h, the cells were washed twice with PBS, and fresh medium was added to each well prior with further incubation at 37°C for 2 d. After washing with PBS, live-cell images were captured under a BZ-X700 phase contrast microscope (Keyence). The cells were then dissolved in 0.2 mol/L NaOH, and the protein content of cell lysates was quantified using a Bio-Rad protein assay kit. Rates of treated cell proliferation were normalized to the proliferation of control cells by the protein level. All in vitro assays were performed simultaneously using 4 replicates in 3 independent experiments.

Biodistribution

^{131}I-IITM or ^{211}At-AITM (1.78 ± 0.11 MBq/0.1 mL) was administrated to B16F10 melanoma–bearing mice via the tail vein. The mice were subsequently sacrificed by cervical dislocation at 1, 2, 6, and 24 h and 3 and 7 d after ^{131}I-IITM injection, or 1, 6, and 24 h after ^{211}At-AITM injection ($n = 4$). Blood, tumor, and major organs were promptly harvested and weighed, and the radioactivities were measured using a γ-counter. The radioactivity of organs and tissues, except the thyroid, is presented as a percentage of the injected dose per gram of wet tissue (%ID/g). That of the thyroid is presented as a percentage of the injected dose (%ID). All radioactivity measurements were corrected for decay.

Therapeutic Effect

B16F10-bearing C57BL/6J mice (body weight, 23.92 ± 0.45 g) with a tumor volume of 0.0431 ± 0.0298 cm^3 were randomly assigned to treatment and control groups. The ^{131}I-IITM therapy study was performed with 3 groups of mice. Mice in the therapy group ($n = 15$) were injected with 18.5 MBq of ^{131}I-IITM, whereas mice in the 2 control groups were injected once weekly for 2 wk with 0.1 mL of either saline ($n = 6$) or 1 mg/kg FITM ($n = 7$).

As a dose-dependent study, we injected normal C57BL/6J mice on a single occasion with ^{211}At-AITM (0, 1.11, 1.85, 3.7, and 7.4 MBq) ($n = 8$ for each dose). To reduce the risk of lethality, the therapeutic efficacy was evaluated by injecting B16F10-bearing C57BL/6J mice with a single administration of ^{211}At-AITM (0, 0.11, 1.11, 1.85, and 2.96 MBq) ($n = 8$ for each dose). Tumor dimensions were measured twice weekly with digital calipers in a blinded manner, and tumor volumes were calculated using the formula (width^2 × length)/2. A tumor volume of 9 cm^3 or body weight loss of more than 20% was considered as the endpoint.

Safety Assessment

Changes in the body weight of mice were evaluated as an indicator of the radiation-related side effects of ^{131}I-IITM or ^{211}At-AITM. The hematology and liver and kidney chemistry of ^{211}At-AITM–treated mice were compared with those of saline-treated mice. Hematologic

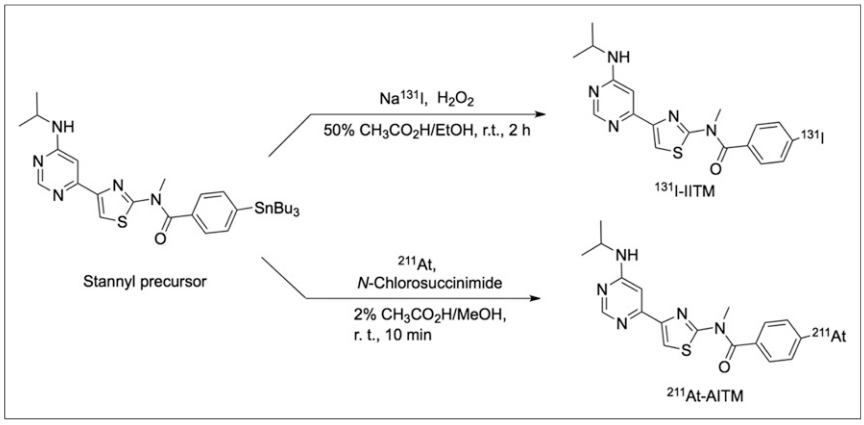

FIGURE 2. Radiosyntheses of ^{131}I-IITM and ^{211}At-AITM.

analyses included leukocyte and platelet counts, which were performed using a Celltack F Automated Hematology Analyzer (Nihon Kohden). Liver and kidney analyses included determinations of aspartate transaminase and alanine transaminase, blood urea nitrogen, and creatinine, which were conducted using Japan Society of Clinical Chemistry reference methods according to the manufacturer's instructions.

Statistical Analysis

Quantitative data are presented as mean ± SD. Intergroup comparisons were performed using an unpaired 2-tailed *t* test or 1-way ANOVA with Dennett's multiple comparison test. The threshold for statistical significance was set at $P < 0.05$.

RESULTS

Radiosynthesis

Radiosynthesis of ^{131}I-IITM or ^{211}At-AITM was assessed by reacting a stannyl precursor with ^{131}I-NaI or ^{211}At (Fig. 2). After semipreparative high-performance liquid chromatography separation from the reaction mixtures, 71–205 MBq of ^{131}I-IITM were obtained in radiochemical yields of 42.7% ± 10.4% ($n = 9$, non–decay-corrected), and 36–118 MBq of ^{211}At-AITM were obtained in yields of 45.7% ± 6.5% ($n = 20$, non–decay-corrected), based on the total radionuclides used. For each batch, the average radiochemical purity of the 2 products exceeded 99% (Supplemental Figs. 1 and 2). ^{131}I-IITM was stable (>97%) in saline and mouse plasma at 37°C for at least 24 h. Similarly, ^{211}At-AITM was stable (97.1% ± 0.8%) in saline, and 78.5% ± 1.0% remained intact after 24-h incubation in mouse plasma.

Binding Ability

^{131}I-IITM displayed a high binding ability to mGluR1-expressing B16F10 melanomas. A dose-dependent increase in radioactivity and maximum uptake (2.5 MBq/mL) of ^{131}I-IITM were observed in mGluR1-expressing melanomas (Supplemental Fig. 3). We thus used 2.5 MBq/mL of ^{131}I-IITM for binding specificity analyses. Considering the high energy of α-radiation, we used 25 kBq/mL of ^{211}At-AITM for binding determinations. The binding specificity of ^{131}I-IITM or ^{211}At-AITM was examined using competitive assays with unlabeled mGluR1-specific FITM (Fig. 3A). The cellular uptake of ^{131}I-IITM and ^{211}At-AITM into B16F10 cells was 22.97% ± 1.50% and 12.87% ± 1.94% ICD/mg protein, respectively, and was significantly decreased to 4.43% ± 0.53% and 1.84% ± 0.46% ICD/mg protein ($P = 0.0041$ and 0.016, respectively) by treatment with FITM. At 1 and 2 h after incubation, ^{211}At-AITM retained in the membrane of B16F10 cells, accounting for 72.24% ± 11.48% and 71.91% ± 8.62% of total bound radioactivity, respectively, and entered into the cell, accounting for 34.65% ± 2.32% and 35.41% ± 3.24% of total radioactivity, respectively. After 18 h, membrane binding had decreased to 19.18% ± 2.52%, whereas the internalized radioactivity had increased to 56.61% ± 11.60% (supplemental materials; Supplemental Fig. 4).

Cytotoxicity

Although ^{131}I-IITM showed a considerably higher degree of binding to B16F10 cells than ^{211}At-AITM at the respective doses (Fig. 3A, $P = 0.03$), we detected no difference in the inhibition of B16F10 cell proliferation after treatment with ^{131}I-IITM or ^{211}At-AITM (60.25% ± 3.80% vs. 62.69% ± 8.74%, $P = 0.74$) when

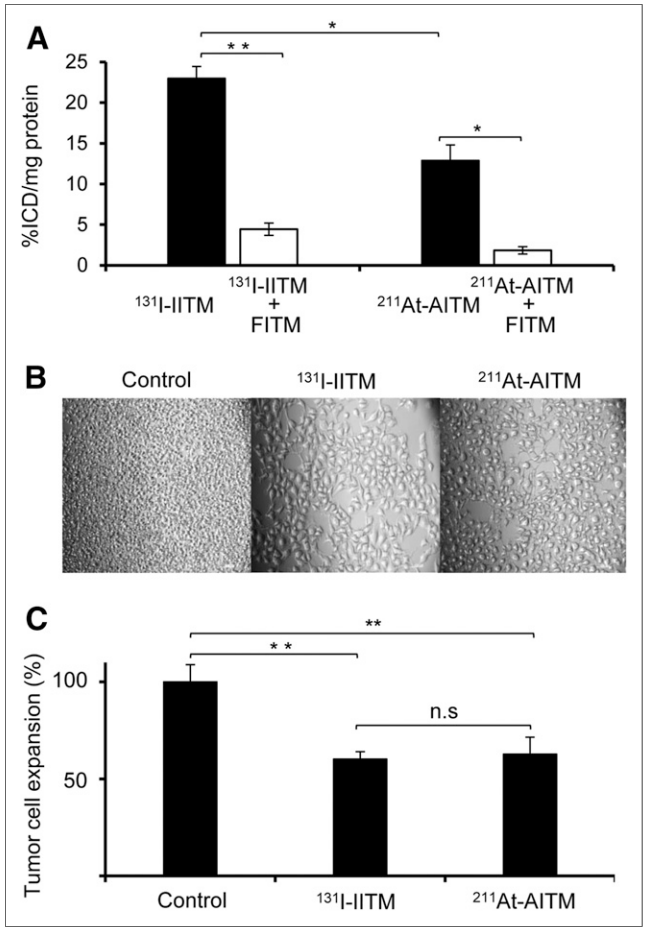

FIGURE 3. In vitro efficacy of ^{131}I-IITM and ^{211}At-AITM. (A) Binding ability and biospecificity of ^{131}I-IITM and ^{211}At-AITM. (B) Representative images of B16F10 cells cultured with medium (control), ^{131}I-IITM, or ^{211}At-AITM. (C) Antiproliferative effect of ^{131}I-IITM or ^{211}At-AITM against B16F10 melanoma cells. Data are expressed as mean ± SD of 3 independent experiments. Intergroup comparisons were performed using unpaired *t* tests. Asterisks indicate statistical significance (*$P < 0.05$, **$P < 0.01$). Scale bars in B represent 0.1 mm.

compared with medium-treated control cells after incubation for 2 d (Figs. 3B and 3C). These results indicated that ^{131}I-IITM and ^{211}At-AITM showed antiproliferative efficacy against mGluR1-expressing B16F10 melanoma.

Biodistribution

Analysis of the in vivo pharmacokinetics of ^{131}I-IITM (Fig. 4 and Supplemental Table 1) indicated that in the mGluR1-positive B16F10 grafts, ^{131}I-IITM showed peak tumor accumulation of radioactivity with 4.66% ± 0.70 %ID/g at 1 h after injection, which remained at 1.05% ± 0.14 %ID/g at 24 h after injection. These results are consistent with the findings of our previous imaging studies (*14,15*). Minimal radioactivity (less than 0.64 % ID/g at all time points) was observed in the brain. Rapid clearance of radioactivity from blood and tissues commenced at 2 h after injection, which could reduce radiation exposure in normal organs. Kidney and gastrointestinal organs exhibited considerably higher levels of radioactivity than other normal organs, indicating that ^{131}I-IITM was cleared through the renal and hepatobiliary routes. Between days 3 and 7 after injection, although a small level of radioactivity was observed in tumor tissues, no considerable amounts of radioactivity were detected in the nontargeted tissues of mice.

On the basis of the observed pharmacokinetics of ^{131}I-IITM and the short half-life of ^{211}At (7.2 h), we selected the early time intervals after injection to determine the in vivo properties of ^{211}At-AITM (Fig. 4 and Supplemental Table 2). Similar pharmacokinetics were found for ^{211}At-AITM. ^{211}At-AITM entered the bloodstream and rapidly reached the targeted tumor with 7.68% ± 0.71 %ID/g at 1 h after injection, which was approximately 2-fold that of ^{131}I-IITM. At all equivalent time points, higher radioactivity was delivered by ^{211}At-AITM into the melanoma grafts than by ^{131}I-IITM ($P < 0.05$). Minimal putative de-astatination was observed in the thyroid (<0.24 %ID) at all time points, whereas the stomach showed high uptake. These biodistribution results indicated that the cytotoxic radionuclides ^{131}I and ^{211}At were carried by the delivery system and effectually transported to the targeted mGluR1-expressing melanomas in vivo. Compared with ^{131}I-IITM, the efficacy of ^{211}At-AITM against melanoma could be enhanced by delivering a higher amount of ^{211}At to the tumor cells.

Therapeutic Efficacy and Safety

The therapeutic efficacy and safety of ^{131}I-IITM were assessed in B16F10-bearing mice (Fig. 5). B16F10 tumors in the saline (control) group grew exponentially from 0.0496 ± 0.01665 cm^3 (pretherapy volume) to 8.95 ± 1.06 cm^3 on day 15. Two doses of ^{131}I-IITM administered 1 wk apart (on days 7 and 14 after B16F10 inoculation) significantly slowed B16F10 tumor growth, resulting in a reduced tumor volume of approximately 61%, compared with the control on day 15 after administration of the initial ^{131}I-IITM dose ($P = 0.0015$). No significant antitumor effect was observed in the FITM group without radionuclide treatment ($P = 0.35$), confirming the specificity of the therapeutic effect of ^{131}I-IITM. Furthermore, no significant changes in body weight or signs of distress were observed in response to ^{131}I-IITM treatment over the experimental period (Fig. 5B).

To derive the safety profile of ^{211}At-AITM in vivo, we performed dose-dependent studies in normal mice using a single administration of increasing doses of ^{211}At-AITM and monitored weight changes and hematologic functions (Fig. 6). All mice treated with 7.4 MBq of ^{211}At-AITM died within 8 d after injection (Fig. 6A). Mice injected with 3.7 MBq of ^{211}At-AITM showed an estimated decrease in body weight of –21.63% at 7 d after injection, and 2 deaths were recorded (Figs. 6A and 6B). There was no significant weight loss in groups administered less than 3.7 MBq (Fig. 6B). Compared with the saline group (Fig. 6C), all mice treated with 1.11–3.7 MBq of ^{211}At-AITM had lower leukocyte counts (29%–38% of initial) at day 2, and the platelet count decreased to 54%–80% of initial at day 7. Although both levels recovered to baseline on day 20, patient management in hematologic functions after ^{211}At-AITM therapy should be considered in the clinical trials. Under these conditions, the lethal dose50 for ^{211}At-AITM was estimated to be 4.02 MBq (Fig. 6A).

All subsequent therapeutic studies were performed with a single injection of ^{211}At-AITM with conservative doses (0–2.96 MBq) to B16F10-bearing C57BL/6J mice. The therapeutic results are summarized in Figure 7. Dose-dependent tumor inhibition was observed in melanoma mice treated with 0.11, 1.11, 1.85, or 2.96 MBq of ^{211}At-AITM

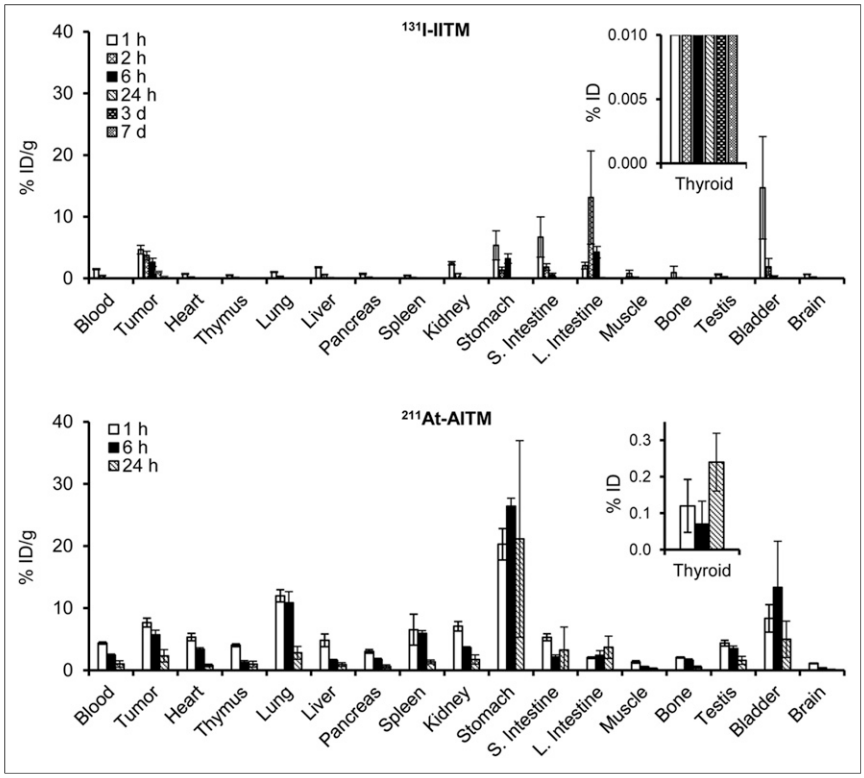

FIGURE 4. Ex vivo biodistribution after the injection of ^{131}I-IITM and ^{211}At-AITM at designated time points in C57BL/6J mice bearing B16F10 melanomas ($n = 4$ for each time point). Data are expressed as mean percentage of the injected radioactivity dose per gram of tissue (%ID/g) ± SD. Note that thyroid values are presented as a percentage of the injected radioactivity dose (%ID). L. Intestine = large intestine; S. Intestine = small intestine.

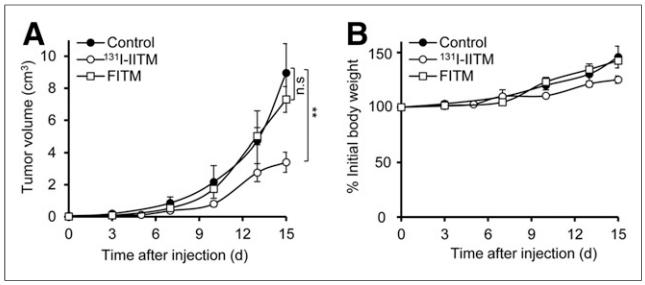

FIGURE 5. Therapeutic efficacy and safety of ^{131}I-IITM in B16F10-bearing C57BL/6J mice. (A) Tumor volumes after treatment. Compared with the control ($n = 6$) and unlabeled FITM ($n = 7$) groups, ^{131}I-IITM ($n = 15$) administration significantly inhibited B16F10 melanoma growth as indicated by tumor size. (B) Changes in body weight. Intergroup comparisons were performed using unpaired 2-tailed t tests. Asterisks indicate statistical significance (**$P < 0.01$). n.s. = no significance.

(Fig. 7A), compared with the 0 MBq (saline)-treated group. A single dose of ^{211}At-AITM (0.11 MBq) resulted in an approximate 32.24% reduction in tumor volume, although this was statistically nonsignificant ($P = 0.09$). Other reductions based on the concentration administered included 73.48% at 1.11 MBq ($P < 0.0001$), 87.38% at 1.85 MBq ($P < 0.0001$), and 95.68% at 2.96 MBq ($P < 0.0001$), compared with the 0 MBq group at 19 d after administration. Overall, the therapeutic efficiency of ^{211}At-AITM was superior to that of ^{131}I-IITM.

The safety of ^{211}At-AITM treatment was monitored in melanoma-bearing mice treated with increasing doses. Throughout the examination period, we observed no decrease in body weight in the melanoma-bearing mice injected with 0–2.96 MBq of ^{211}At-AITM (Fig. 7B). Given the temporarily high radioactivity during renal and hepatobiliary excretion of ^{211}At-AITM, we examined the potential of liver or kidney damage. Liver function was evaluated by measuring aspartate transaminase and alanine transaminase, whereas kidney function was evaluated by measuring blood urea nitrogen and creatinine using the sera of melanoma-bearing mice treated with 0 or 2.96 MBq of ^{211}At-AITM. As shown in Figure 7C, compared with 0 MBq, there were no significant changes in the levels of liver and kidney enzymes on days 1 and 7 after exposure to 2.96 MBq α-radiation. Accordingly, we verified that ^{211}At-AITM has high therapeutic efficiency with minimal health risks.

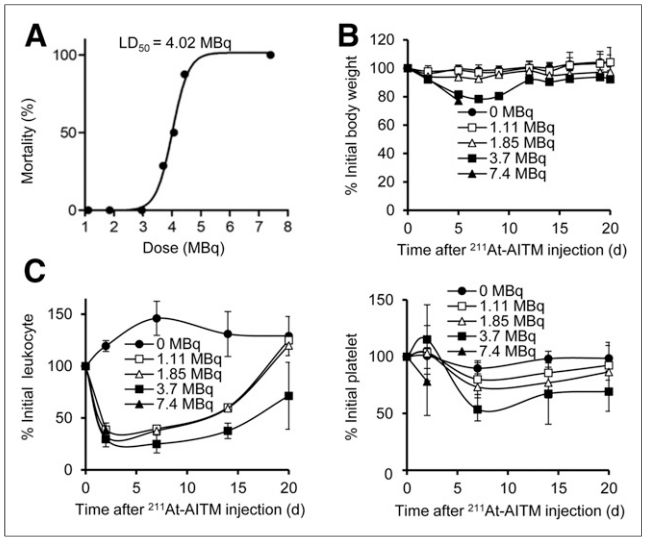

FIGURE 6. Safe ^{211}At-AITM dosage for normal C57BL/6J mice. (A) LD_{50} values of ^{211}At-AITM. A dose-dependent study was performed by administering a single dose of ^{211}At-AITM (0–7.4 MBq) to normal mice. All mice survived when a dose of less than 3.7 MBq ^{211}At-AITM was administered via injection. (B) Changes in body weight. (C) Changes in leukocyte and platelet counts. Data are expressed as mean ± SD, respectively ($n = 8$). LD_{50} = lethal dose50.

DISCUSSION

Several factors must be taken into consideration when developing an effective TRT radiopharmaceutical, including the selections of targeted receptor, radionuclide, and carrier (*3,8*). By focusing on these critical components, we designed and synthesized 2 small-molecule radiopharmaceuticals, ^{131}I-IITM and ^{211}At-AITM, to target the oncoprotein mGluR1 that is overexpressed in melanomas. We accordingly demonstrated that delivery of the radionuclides ^{211}At and ^{131}I via small molecular carriers resulted in marked tumor growth inhibition in mGluR1-expressing melanoma-bearing mice without significant side effects.

An ideal target receptor is one that is generally expressed on the surface of tumor cells, rather than within the cytoplasm or nucleus (*8*). In the present study, we selected the cell surface–expressing receptor mGluR1, which is not expressed by normal melanocytes or benign nevi, but is highly and specifically expressed in melanoma (*9,10*). Thus, this oncoprotein can be targeted with a high concentration of TRT radiopharmaceuticals delivered to malignant cell surfaces. Herein, we successfully synthesized ^{131}I-IITM and ^{211}At-AITM with sufficient radioactivity, radiochemical yield, and purity for evaluation studies (Fig. 2). Although mGluR1 also occurs in brain tissue, neither of the assessed radiopharmaceuticals penetrated the blood–brain barrier to bind with brain mGluR1, whereas we observed high and rapid uptake by tumors (Fig. 4). The mean doses per unit of injected activity (grays per MBq) of β-disintegrations from ^{131}I-IITM and α-disintegrations from ^{211}At-AITM absorbed by tumors were estimated based on a standard method using the MIRD formula (*16*). The radiation doses absorbed by tumors were 2.68 Gy/MBq for ^{131}I-IITM and 4.22 Gy/MBq for ^{211}At-AITM, respectively.

Optimization of TRT radiopharmaceuticals requires consideration of the nature of specific radionuclides and the overall intended application. Given that β-emitting radiopharmaceuticals may destroy neighboring nontarget tumor cells through the "crossfire" effect (*17*), we initially developed ^{131}I-IITM targeting mGluR1. The cytotoxic effects of ^{131}I-IITM were examined in vitro and in vivo, and we accordingly verified significant antitumor effects in the mGluR1-expressing B16F10 cells (Fig. 3) and melanoma-bearing mice after ^{131}I-IITM administration (Fig. 5). Given that melanomas are generally recognized as being radiation resistant, our tumor growth inhibition data for ^{131}I-IITM are particularly impressive (*18*). With respect to the treatment of microscopic or small-volume melanomas, we further used the α-emitting ^{211}At to synthesize ^{211}At-AITM, which would be preferable for killing isolated tumor cells without damaging normal tissues, as α-radiation produced by ^{211}At decay has a high linear energy of 6.8 MeV and acts over a short range of approximately 50–100 μm (vs. several mm for β particles) (*19*). Therefore, ^{211}At-AITM, targeting the small molecule mGluR1, was very effective in the treatment of murine melanomas (Figs. 3 and 7A). Moreover, the therapeutic effects of ^{211}At-AITM in the B16F10-bearing mice were dose-dependent, and we observed no severe side effects in normal organs (Fig. 7). This demonstrated the superior therapeutic efficiency of

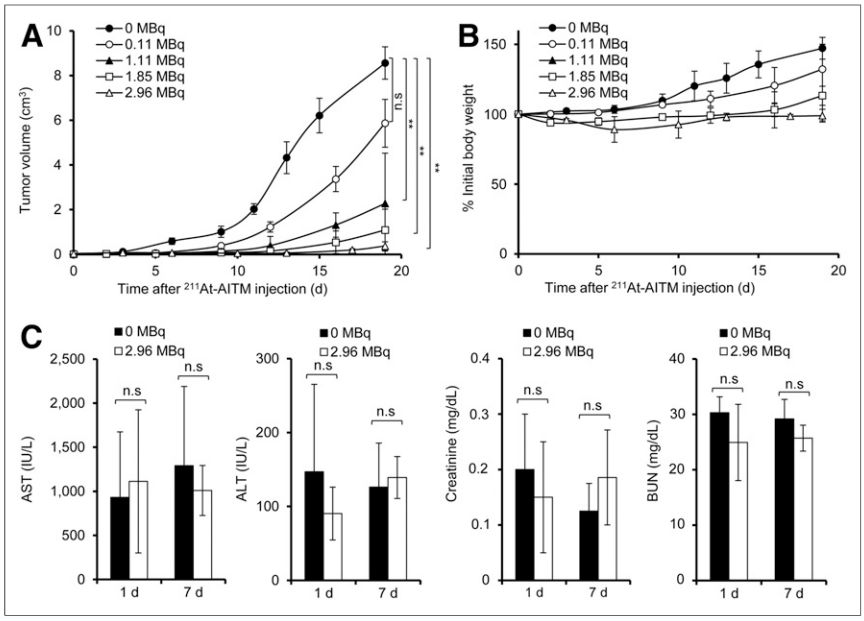

FIGURE 7. Therapeutic efficacy and safety of ^{211}At-AITM in B16F10-bearing C57BL/6J mice. (A) Tumor volumes after ^{211}At-AITM treatment. Dose-dependent tumor inhibition was observed in melanoma-bearing mice treated with different doses of ^{211}At-AITM, compared with mice administered 0 MBq. (B) Changes in body weight. (C) AST, ALT, creatinine, and BUN values. Liver function was evaluated by measuring AST and ALT, and kidney function by measuring BUN and creatinine in the sera of melanoma-bearing mice administered 0 or 2.96 MBq of ^{211}At-AITM. Intergroup comparisons were performed using unpaired 2-tailed *t* tests or 1-way ANOVA with Dunnett's multiple comparison test. Data are expressed as mean ± SD, respectively (n = 8). Asterisks indicate statistical significance (**P < 0.01). ALT = alanine transaminase; AST = aspartate transaminase; BUN = blood urea nitrogen; n.s. = no significance.

^{211}At-AITM, compared with ^{131}I-IITM in the mGluR1-expressing melanoma model.

Our in vivo evaluations revealed that at 24 h after ^{131}I-IITM and ^{211}At-AITM injection, large quantities of ^{131}I and ^{211}At had been delivered to the melanoma-associated mGluR1 target, with peak tumor uptake observed at 1 h after injection (Fig. 4). Clearance of the remaining unbound radioactivity from the blood and whole body, via the renal and hepatobiliary routes, commenced within 2 h. In this regard, it is important to note that the temporarily high radioactivity in the blood, kidneys, and gastrointestinal tract did not induce weight reduction, severe hematologic toxicity, or apparent functional side effects in the liver and kidney after ^{131}I-IITM or ^{211}At-AITM administration (Figs. 5B, 6C, and 7C). These results indicate that ^{131}I-IITM and ^{211}At-AITM could be safely delivered to mGluR1-expressing tumors with negligible radiotoxicity. Despite the rapid whole-body clearance of the small-molecule carriers, there was no obvious decrease in delivery efficiency to the cancerous organs (Fig. 4). Given that the established pharmacokinetics indicate the feasibility of delivering both long-lasting β-emitting nuclides and short-lived α-emitting nuclides, we believe that the newly developed radiopharmaceuticals will make a valuable contribution to mGluR1-based TRT studies.

This study does, nevertheless, have certain limitations. Although we obtained encouraging therapeutic results for TRT using ^{131}I-IITM and ^{211}At-AITM in a B16F10 melanoma model, not all malignant cells were eliminated in our initial evaluation of therapeutic effects and side effects according to the empiric protocol of ^{131}I- and ^{211}At-labeled compounds. In the present protocols, we administered 2 doses of ^{131}I-IITM 1 wk apart, whereas only a single dose of ^{211}At-AITM was administered. Using safe doses, multiple-dose administrations of ^{131}I-IITM and ^{211}At-AITM could be directly applied to enhance therapeutic efficacy with acceptable toxicity.

CONCLUSION

We successfully developed ^{131}I-IITM and ^{211}At-AITM as 2 novel radiopharmaceuticals for oncoprotein mGluR1-based TRT studies of melanoma. Both radiopharmaceuticals were synthesized with sufficient radioactivity, radiochemical yield, and purity. Their rapid uptake and stable retention in tumors and extremely rapid blood and whole-body clearance facilitated strong tumor growth inhibition with negligible side effects in a mGluR1-expressing melanoma model. Using a TRT approach, these small-molecule radiopharmaceuticals allow effective treatment of melanomas. Moreover, the properties of these radiopharmaceuticals indicate the possibility of combining imaging and TRT studies to construct a framework of precision cancer treatment targeting the oncoprotein mGluR1.

DISCLOSURE

This work was supported in part by the JSPS KAKENHI (grant nos. 17H04267, 17K16495) and the initiative for realizing diversity in the research environment. No other potential conflict of interest relevant to this article was reported.

ACKNOWLEDGMENTS

We thank the staff at QST for their technical support in radionuclide production, radiosynthesis, and animal experiments.

KEY POINTS

QUESTION: How well do small-molecule radiopharmaceuticals targeting oncoprotein mGluR1 function as TRT agents for melanoma therapy?

PERTINENT FINDINGS: We developed 2 small-molecule radiopharmaceuticals, ^{131}I-IITM and ^{211}At-AITM, to target the oncoprotein mGluR1 in melanomas. Both radiopharmaceuticals precisely and safely deliver therapeutic radionuclides to the targeted melanomas, resulting in marked tumor growth inhibition in mGluR1-expressing melanoma-bearing mice, without significant side effects.

IMPLICATIONS FOR PATIENT CARE: Our findings indicate that ^{211}At-AITM and ^{131}I-IITM can be developed clinically as high-precision TRT agents targeting the oncoprotein mGluR1, thereby indicating the potential of using the TRT approach to improve the outcomes of patients with melanomas.

REFERENCES

1. Gill MR, Falzone N, Du Y, Vallis KA. Targeted radionuclide therapy in combined-modality regimens. *Lancet Oncol.* 2017;18:e414–e423.

2. Jackson MR, Falzone N, Vallis KA. Advances in anticancer radiopharmaceuticals. *Clin Oncol (R Coll Radiol).* 2013;25:604–609.
3. Kassis AI, Adelstein SJ. Radiobiologic principles in radionuclide therapy. *J Nucl Med.* 2005;46(suppl 1):4S–12S.
4. Jhanwar YS, Divgi C. Current status of therapy of solid tumors. *J Nucl Med.* 2005;46(suppl 1):141S–150S.
5. Guryev EL, Volodina NO, Shilyagina NY, et al. Radioactive (^{90}Y) upconversion nanoparticles conjugated with recombinant targeted toxin for synergistic nanotheranostics of cancer. *Proc Natl Acad Sci USA.* 2018;115:9690–9695.
6. Li HK, Morokoshi Y, Nagatsu K, Kamada T, Hasegawa S. Locoregional therapy with α-emitting trastuzumab against peritoneal metastasis of human epidermal growth factor receptor 2-positive gastric cancer in mice. *Cancer Sci.* 2017;108:1648–1656.
7. Janik JE, Morris JC, O'Mahony D, et al. ^{90}Y-daclizumab, an anti-CD25 monoclonal antibody, provided responses in 50% of patients with relapsed Hodgkin's lymphoma. *Proc Natl Acad Sci USA.* 2015;112:13045–13050.
8. Srinivasarao M, Galliford CV, Low PS. Principles in the design of ligand-targeted cancer therapeutics and imaging agents. *Nat Rev Drug Discov.* 2015;14:203–219.
9. Pollock PM, Cohen-Solal K, Sood R, et al. Melanoma mouse model implicates metabotropic glutamate signaling in melanocytic neoplasia. *Nat Genet.* 2003;34:108–112.
10. Namkoong J, Shin SS, Lee HJ, et al. Metabotropic glutamate receptor 1 and glutamate signaling in human melanoma. *Cancer Res.* 2007;67:2298–2305.
11. Prickett TD, Samuels Y. Molecular pathways: dysregulated glutamatergic signaling pathways in cancer. *Clin Cancer Res.* 2012;18:4240–4246.
12. Yamasaki T, Fujinaga M, Kawamura K, et al. In vivo measurement of the affinity and density of metabotropic glutamate receptor subtype 1 in rat brain using ^{18}F-FITM in small-animal PET. *J Nucl Med.* 2012;53:1601–1607.
13. Yamasaki T, Fujinaga M, Yoshida Y, et al. Radiosynthesis and preliminary evaluation of 4-[^{18}F]fluoro-*N*-[4-[6-(isopropylamino)pyrimidin-4-yl]-1,3-thiazol-2-yl]-*N*-methylbenzamide as a new positron emission tomography ligand for metabotropic glutamate receptor subtype 1. *Bioorg Med Chem Lett.* 2011;21:2998–3001.
14. Xie L, Yui J, Fujinaga M, et al. Molecular imaging of ectopic metabotropic glutamate 1 receptor in melanoma with a positron emission tomography radioprobe ^{18}F-FITM. *Int J Cancer.* 2014;135:1852–1859.
15. Fujinaga M, Xie L, Yamasaki T, et al. Synthesis and evaluation of 4-halogeno-*N*-[4-[6-(isopropylamino)pyrimidin-4-yl]-1,3-thiazol-2-yl]-*N*-[^{11}C]methylbenzamide for imaging of metabotropic glutamate 1 receptor in melanoma. *J Med Chem.* 2015;58:1513–1523.
16. Stabin MG. Mirdose: personal computer software for internal dose assessment in nuclear medicine. *J Nucl Med.* 1996;37:538–546.
17. Jadvar H. Targeted radionuclide therapy: an evolution toward precision cancer treatment. *AJR.* 2017;209:277–288.
18. Barranco SC, Romsdahl MM, Humphrey RM. The radiation response of human malignant melanoma cells grown in vitro. *Cancer Res.* 1971;31:830–833.
19. Mulford DA, Scheinberg DA, Jurcic JG. The promise of targeted {alpha}-particle therapy. *J Nucl Med.* 2005;46(suppl 1):199S–204S.